http://dx.doi.org/10.14500/aro.12248

Artificial Intelligence - Based Digital Pathology Assessment of CD44s Expression in Breast Cancer: Association with Clinicopathological Features and Survival Outcomes

Avan S. Mohammed[1†], Ramadhan T. Othman[2] and Rafil T. Yaqo[3]

[1]Department of Biology, Faculty of Science, University of Duhok, Duhok, Kurdistan Region – F.R. Iraq

[2]Department of Medicine, College of Medicine, University of Duhok, Duhok, Kurdistan Region – F.R. Iraq

[3]Department of Pathology, College of Medicine, University of Duhok, Duhok, Kurdistan Region – F.R. Iraq

***Abstract*—Breast cancer (BC) exhibits considerable molecular and clinical heterogeneity, complicating prognostic evaluation. The cluster of differentiation 44 standard (CD44s) isoform has been proposed as a prognostic marker in various cancers; however, its role in BC remains unclear. This study evaluated CD44s expression in BC tissues and its association with clinicopathological features and survival outcomes using an artificial intelligence (AI)-based digital pathology scoring method. A retrospective analysis of 98 BC tissue samples is conducted, with CD44s cell membrane protein expression assessed through both manual and AI-based immunohistochemical (IHC) scoring. Statistical analyses included Pearson's chi-square test, Kaplan-Meier (log-rank), and Cox regression. CD44s expression was observed in 65.31% of patients. No significant associations are found between CD44s expression and clinicopathological characteristics, including age, tumor size, lymph node metastasis, histological grade, lymphovascular invasion (LVI), or hormone receptor status (all $p > 0.05$). Survival analysis reveals no significant association between CD44s expression and overall survival (OS, $p = 0.1345$) or progression-free survival ($p = 0.0669$). While CD44s expression is prevalent in BC samples, it is not an independent prognostic factor; LVI is the only significant predictor of OS ($p = 0.036$). Finally, the moderate agreement between AI and manual scoring (Cohen's Kappa = 0.4337, $p < 0.0001$) supports the potential of AI-assisted methods for biomarker quantification, warranting further validation in larger cohorts.**

***Index Terms*—Artificial intelligence, Breast cancer stem cells, Breast cancer, CD44s, Immunohistochemistry, QuantCenter.**

ARO-The Scientific Journal of Koya University
Vol. XIII, No. 1 (2025), Article ID: ARO.12248. 9 pages
DOI: 10.14500/aro.12248
Received: 04 May 2025; Accepted: 02 June 2025
Regular research paper; Published: 22 June 2025
†Corresponding author's e-mail: avan.mohammed@uod.ac

I. Introduction

Breast cancer (BC) is the primary cause of mortality among females. Global figures indicate that around 9.7 million new cancer cases were diagnosed in females in 2022, with BC comprising 23.8% of all cases, far surpassing lung cancer at 9.4% (Bray, et al., 2024). In Iraq, BC exhibits a 23.1% incidence rate, and a 15.7% mortality rate compared to other malignancies, making it the country with the highest prevalence and fatality rates for BC in the Middle East (Zahwe, et al., 2025). The occurrence of BC and the potential for later recurrence or metastasis are caused by several risk factors. These include age, genetic profile, reproductive characteristics, obesity, alcohol consumption, smoking, and general lifestyle choices. In addition, intrinsic molecular subtypes of BC, based on tumor gene expression and phenotypes, are also considered risk factors in the disease etiology (Barnard, Boeke and Tamimi, 2015; Winters, et al., 2017; Lee, et al., 2019). BC is a heterogeneous disease with variability in both clinical and molecular characteristics, which results in differing responses to treatments (Turner, et al., 2021).

Cancer stem cells (CSCs) represent a small subset of cancer cells that exhibit self-renewal, differentiation, and tumorigenic capabilities. They also have the ability to undergo epithelial-to-mesenchymal transition, which substantially contributes to tumor heterogeneity, leading to therapeutic resistance and an increased chance of local recurrences and metastasis (Walcher, et al., 2020; Wilson, et al., 2020). The cluster of differentiation 44 (CD44) is a transmembrane glycoprotein expressed on several human cell types, including embryonic stem cells, immune cells, and connective tissues (Goodison, Urquidi and Tarin, 1999). CD44 is recognized as a molecular marker of CSCs (Al-Hajj, et al., 2003; Schmitt, et al., 2012). This gene regularly undergoes alternative splicing, which results in the standard (CD44s) and variable (CD44v) isoforms (Wilson, et al.,

2020). CD44 interaction with extracellular ligand activates various signaling pathways leading to cell proliferation, survival, adhesion, invasion, and migration (Herrera-Gayol and Jothy, 1999; Senbanjo and Chellaiah, 2017).

In BC, CD44 plays an essential role in tumor aggressiveness, progression, and the induction of CSC traits (Lopez, et al., 2005; Vadhan, et al., 2022; Gu, et al., 2022; Zhang, et al., 2019). Despite the recent advancements in BC therapy, certain patients experience disease recurrence. This may be attributed to the existence of BC stem cells (BCSCs) that withstand chemotherapy and radiotherapy (Steinbichler, et al., 2018; Clark, et al., 2022). Nevertheless, conflicting results concerning stemness and carcinogenesis were observed based on various splice variants of CD44 (Cho, et al., 2015; Zhang, et al., 2019). A study reported that the lack of CD44s correlates with a high incidence of lymph node metastases and poorer prognoses in BC patients (Gong, et al., 2005). In the triple-negative BC (TNBC) molecular subtype, CD44 was found to be related to the aggressiveness and resistance to the targeted therapy when transformed from the standard isoform into the variant isoform (Bei, et al., 2020). The mechanisms through which CD44s influence BC remain ambiguous. Precise histological diagnosis, molecular subtyping, and further classification are essential to better understand the causes of mortality and morbidity associated with this disease. In recent years, the application of artificial intelligence (AI) has attracted increasing interest in BC diagnostics, particularly in the evaluation of immunohistochemistry (IHC) and molecular markers. Conventional IHC assessments depend heavily on manual evaluation by pathologists, a process that is inherently subjective and prone to inter- and intra-observer variability. AI-driven approaches provide a more objective, consistent, and high-throughput alternative for interpreting IHC results (Rakha, Vougas and Tan, 2022; Pati, et al., 2024). These systems have shown promise in analyzing key biomarkers such as estrogen receptor (ER), progesterone receptor (PR), human epidermal growth factor receptor 2 (HER2), and the Ki-67 index, as well as BCSC markers, such as CD44, thereby enhancing diagnostic accuracy and assisting clinicians in selecting the most appropriate treatment in a timely manner (Wu, et al., 2023; McCaffrey, et al., 2024; Xiong, et al., 2025). Therefore, this study was designed to apply AI-based digital pathology (DP) to evaluate CD44s IHC expression in BC patients, aiming to assess its correlation with clinicopathological features, molecular subtypes, and survival, as well as to examine its prognostic and predictive value.

II. Materials and Methods

A. Sample Collection

The present retrospective study was approved by the Directorate of Health Research Ethics Committee through the College of Science-Biology Department, University of Duhok (Number: 21082022-6-5). A total of 105 formalin-fixed paraffin-embedded (FFPE) BC tissue blocks of patients who underwent surgery (from 2013 to 2019) were collected from the Histopathology Departments of both the Central Laboratory and Vajeen Private Laboratory in Duhok Province. Medical records and histopathological data were retrieved from both laboratories' databases and the medical oncology department at Azadi Cancer Center/Duhok/Iraq. All patients received routine chemotherapy, radiotherapy, and/or hormonal therapy following surgery according to the stage of the disease. The retrieved clinicopathological data were the age at diagnosis, pathological diagnosis of BC, histological grade, tumor size, axillary lymph node metastasis status, tumor stage, distance metastasis, and hormonal status such as ER and PR, HER2 expression, and the proliferative marker (Ki-67).

The classification of BC molecular subtypes was conducted according to the IHC profile, based on ER, PR, HER2, and the Ki-67 index, using a 20% cutoff to distinguish between high and low expression levels (Dai, et al., 2015; Bustreo, et al., 2016). In this study, the defined molecular subtypes of BC were as follows: luminal A (ER+, PR+, HER2-, Ki-67 <20%), luminal B HER2-negative (ER+, PR+, HER2-, Ki-67 ≥20%), luminal B HER2-positive (ER+, PR+, HER2+, any Ki-67), HER2-enriched (ER-, PR-, HER2+, Ki-67 ≥20%), and TNBC (ER-, PR-, HER2, Ki-67 ≥20%) (Vallejos, et al., 2010; Somal, et al., 2023).

In this study, the exclusion criteria included fine needle aspiration samples and core biopsies; only cases with excisional biopsies were included. Patients diagnosed with stage IV disease and those who were lost to follow-up were also excluded. All patients were followed every 6 months during the study period through phone calls, and survival data were validated using hospital records, pathology reports, and oncology follow-up records. Tumor grading was defined according to the combined Bloom–Richardson grading system (Elston and Ellis, 1991), and tumor staging was based on the International Union Against Cancer–American Joint Committee on Cancer TNM criteria (Giuliano, Edge and Hortobagyi, 2018). Overall survival (OS) was defined as the time from the date of surgery to death, while progression-free survival (PFS) was defined as the time from diagnosis to the first progression event.

B. IHC Staining of CD44s

IHC slides were prepared from three-micron sections cut from corresponding FFPE blocks. Heat-induced epitope retrieval was used for dewaxing and hydration at 50–60°C overnight (Paulsen, Dimke and Frische, 2015). Antigen retrieval was then performed using a water bath method (Dako, PT Link). Slides were placed in a water bath containing 1.5 L of low pH (×50) Target Retrieval Solution (Dako, EnVision™ FLEX; K8005, Glostrup, Denmark), following a specific protocol with a pre-heat temperature of 65°C and antigen retrieval at 97°C for 20 min. Afterward, the slides were immediately transferred to the PT Link Rinse Station containing diluted wash buffer (PBS ×20) (Dako, EnVision™ FLEX; K8000, Glostrup, Denmark) at room temperature for 1–5 min to prevent dehydration.

The IHC staining was performed using the Dako Autostainer Link 48 and a polymer-based detection system, following the recommended antibody protocol. All reagents were from the Dako EnVision™ FLEX Visualization Kit (K8000). To detect the CD44s cell membrane protein, a monoclonal mouse anti-human CD44s antibody (clone DF1485; Dako, Glostrup, Denmark) was used at a dilution of 1:50, prepared by mixing 1 μL of the concentrated antibody with 49 μL of antibody diluent.

The staining procedure consisted of several steps. First, endogenous peroxidase activity and non-specific binding were blocked using a peroxidase blocking reagent for 5 min. The primary antibody was then applied and incubated for 20 min. This was followed by rinsing in wash buffer and incubation with the secondary FLEX+ Mouse (LINKER) reagent for 15 min. After another rinse, slides were incubated in EnVision FLEX/HRP for 20 min, followed by two additional washes. To visualize antigen staining, 3,3'-diaminobenzidine was applied, and the slides were counterstained with hematoxylin. Finally, the slides were dehydrated through graded ethanol (70–100%) and mounted using Dibutyl-phthalate Polystyrene Xylene. Human urinary bladder tissue was used as a positive control for each sample.

C. Digitizing the Slides and Utilizing AI for Evaluation through DP/3DHISTECH

The prepared CD44s IHC slides were initially digitized using the Pannoramic® Desk II DW scanner from 3DHISTECH (Budapest, Hungary). SlideViewer 2.5, a digital microscopy tool, was subsequently used to examine the scanned slides. The certified QuantCenter 2.3 Image Analyzer was then employed to quantify the CD44s transmembrane protein (User Guide, June 3, 2021; MembraneQuant Image Analyzer) (Acs, et al., 2019; Braun, et al., 2020). The "PatternQuant" module was first selected to identify specific malignant and stromal regions. Subsequently, "MembraneQuant" color deconvolution was applied within the delineated malignant regions, based on the chromogen color of the marker.

The image analysis procedure uses quantitative algorithms that mimic the pathologist's assessment, producing semiquantitative outcomes on a non-standardized scoring system. Cell membranes are colored blue, yellow, orange, or red, corresponding to final scores of 0–+3, respectively. The final score is determined based on both the percentage of positive cells within the malignant area and the staining intensity (Aeffner, et al., 2018; Liu, et al., 2023). To validate the AI-based scoring by DP/3DHISTECH, the IHC slides were also manually evaluated by two pathologists.

D. Manual Scoring

Manual scoring was performed on the same digitized slides by two pathologists who were blinded to the patients' clinicopathological data. For each slide, five fields were examined using SlideViewer 2.5 at ×20 magnification. CD44s expression was evaluated based on the percentage of positive cells (0 points: <5%; 1 point: 6–25%; 2 points: 26–50%; 3 points: 51–75%; and 4 points: 76–100%) and the staining intensity of the cell membrane (0 points: no staining; 1 point: weak staining; 2 points: moderate staining; and 3 points: strong staining). The final score was calculated by multiplying the percentage score by the intensity score, yielding a total score ranging from 0 to 12. A score of ≥3 was considered positive (Wu, et al., 2015).

E. Statistical Methods

The general and medical characteristics of BC patients were presented as mean (SD), median (median absolute deviation [MAD]), or percentages. The association between CD44s protein expression and clinicopathological data was examined using the Pearson Chi-square test. The Kaplan-Meier method was used for OS and PFS analysis. Comparisons of OS and PFS across different general and medical characteristics were performed using the Wilcoxon/Kruskal–Wallis test (rank sums test). Cox regression analysis, based on the proportional hazards model, was conducted to identify factors associated with OS and PFS, considering mortality as the outcome. The strength and precision of these associations were expressed as hazard ratios (HR) with 95% confidence intervals (CI). Cohen's Kappa test was used to assess the agreement between manual scoring and AI-based scoring of CD44s protein expression. A $p < 0.05$ was considered statistically significant. All statistical analyses were performed using JMP®, Version 18.0 (SAS Institute Inc., Cary, NC, 1989–2023).

III. Results

A. Patient Baseline Characteristics

In this study, a total of 105 BC samples were obtained, of which 98 were included in the analysis, while 7 cases were excluded due to loss to follow-up. All of the included samples were invasive ductal carcinoma. The patients' clinicopathological characteristics are listed in Table I. The mean age at diagnosis was 48.36 ± 11.28 years (range: 28–75 years), with the majority of patients (72.45%) being over 40 years old. Regarding tumor size, 68.37% of patients had tumors measuring >2 cm to ≤5 cm, 18.37% had tumors >5 cm, and 13.27% had tumors ≤2 cm. Histological grading revealed that 54.08% of patients had Grade III tumors, 41.84% had Grade II, and 4.08% had Grade I. TNM cancer staging results were as follows: Stage II (50%), Stage III (39.8%), and Stage I (10.2%). Lymph node metastasis was present in 65.31% of patients, while 34.69% had no lymph node involvement. Lymphovascular invasion (LVI) was observed in 74.23% of cases. In addition, 11.22% of patients developed local recurrence, and 13.27% developed distant metastases. Metastatic patterns were identified in the bone and vertebrae (3 cases), head and brain (5 cases), liver (2 cases), peritoneum (1 case), skin (1 case), and one case with an unidentified metastatic site.

In the present study, the ER, PR, and HER2 status of BC patients was categorized into positive and negative groups. The ER and PR status results were identical, with

70.41% of patients testing positive and 29.59% testing negative. Regarding HER2 status, 30.61% of patients were HER2-positive, while 69.39% were HER2-negative. Fifty-three patients (54.08%) had a Ki-67 index score of ≥20, while forty-five patients (45.92%) had a score of <20. The molecular classification of BC cases identified Luminal A as the most prevalent subtype, comprising 38 cases (38.78% of the cohort). This was followed by Luminal B HER2-negative with 21 cases (21.65%) and HER2-enriched with 18 cases (18.56%). The remaining subtypes included Luminal B HER2-positive (11 cases, 11.34%) and TNBC, the least common subtype, with 9 cases (9.28%).

B. CD44s Protein Expression

CD44s is predominantly expressed in the cell membranes of BC tissues, as illustrated in Fig. 1. CD44s protein expression, as determined by AI scoring, was positive in 65.31% of patients and negative in 34.69%. The agreement between AI and manual scoring was moderate, with a Cohen's Kappa value of 0.4337 ($p < 0.0001$).

C. Association between CD44s Expression and Clinicopathological Features

This study analyzed the association between clinicopathological characteristics and the expression of the CD44s cell membrane protein (Table I). CD44s positivity was higher in patients over 40 years of age (74.07%) compared to those aged ≤40 years (61.97%), although this difference was not statistically significant ($p = 0.2608$). Similarly, CD44s expression showed no significant association with tumor size, lymph node metastasis, histological grade, LVI, or disease stage ($p = 0.8904$; $p = 0.2126$; $p = 0.7385$; $p = 0.1789$; $p = 0.6946$, respectively).

In terms of hormone receptor status, CD44s positivity was higher in ER-negative and PR-negative patients (75.86%) compared to ER-positive and PR-positive patients (60.87%); however, these differences were not statistically significant ($p = 0.1547$ for both). For HER2 status, CD44s positivity was greater in HER2-positive patients (73.33%) than in HER2-negative patients (61.76%), but this difference was not statistically significant ($p = 0.2675$). The Ki-67 index showed that CD44s positivity was higher in patients with a Ki-67 index ≥20% (73.58%) than in those with <20% (55.56%), although the difference was not statistically significant ($p = 0.0617$).

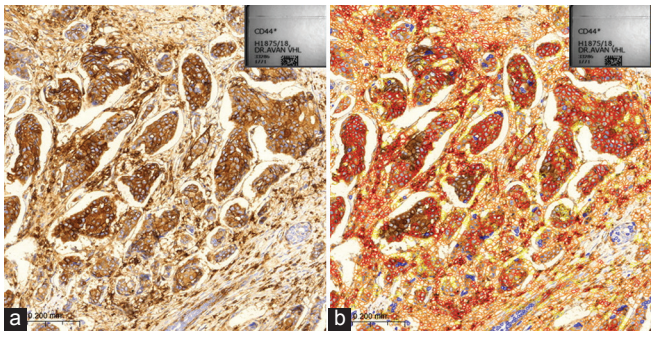

Fig. 1. Representative digital pathology images (3DHISTECH). (a) Scanned IHC slide illustrating CD44s protein expression in breast cancer tissue, visualized using SlideViewer. (b) QuantCenter software performing color deconvolution of immunohistochemical staining for CD44s cell membrane protein expression. Blue indicates absence of membrane staining (score 0), while yellow, orange, and red represent increasing staining intensities, corresponding to scores of +1, +2, and +3, respectively.

Regarding molecular subtypes, CD44s expression varied among subtypes but did not reach statistical significance ($p = 0.251$). Notably, the highest expression was observed in the HER2-Enriched subtype (78.95%) and Luminal-B HER2-negative (76.19%), followed by TNBC (66.67%) and Luminal-B HER2-positive (63.64%), while the lowest expression was seen in the Luminal-A subtype (52.63%).

Progression events such as local recurrence, distant metastasis, or death were more frequent in CD44s-positive cases (74.36%) compared to those with no progression (59.32%), although the difference was not statistically significant ($p = 0.126$). Local recurrence specifically demonstrated a higher rate of CD44s expression (90.91%) compared to non-recurrent cases (62.07%), though this difference also did not reach statistical significance ($p = 0.058$). Similarly, distant metastasis showed no significant association with CD44s expression (61.54% in metastatic cases vs. 65.88% in non-metastatic cases; $p = 0.759$). Finally, no significant survival difference was observed between CD44s-positive and CD44s-negative groups ($p = 0.202$).

D. Survival Analysis

Kaplan-Meier analysis, including the log-rank test, was used to assess OS and PFS across various BC patient characteristics. Median OS and median PFS are reported in months, along with the MAD (Table II). Patients with tumors measuring >2–≤5 cm had a median OS of 86.47 months (MAD = 15.86), which was significantly longer than that of patients with tumors >5 cm (median OS = 53.42 months, MAD = 25.39; $p = 0.0229$). Similarly, PFS was significantly longer for patients with tumors ≤2 cm (median PFS = 86.7 months, MAD = 18.53) compared to those with tumors >5 cm (median PFS = 17.85 months; $p = 0.0023$).

Stage I disease was associated with the longest survival, with a median OS of 87.05 months (MAD = 20.44) and a median PFS of 87.05 months (MAD = 20.44). A significant difference in PFS was observed across disease stages ($p = 0.0199$). In addition, ER and PR status significantly impacted both OS and PFS. ER-positive and PR-positive patients had longer median OS (86.33 months) and PFS (75.9 months) compared to ER-negative and PR-negative patients (median OS = 69.4 months, $p = 0.0198$; median PFS = 61.23 months, $p = 0.0392$).

Among the molecular subtypes of BC, Luminal-B HER2-negative tumors demonstrated the longest median OS at 87.4 months (MAD = 11.4), whereas HER2-Enriched tumors exhibited the shortest median OS at 68.5 months (MAD = 27.27), although this difference approached but did not reach statistical significance ($p = 0.0982$). Similarly, PFS was longer in Luminal-B HER2-negative cases, with a

 http://dx.doi.org/10.14500/aro.12248

TABLE I
General Medical and Clinicopathological Characteristics of BC Patients and their Association with AI-based Scores of CD44s Protein Expression

Characteristics	Categories, n (%)		CD44s protein expression, n (%)		p-value
			Negative 34 (34.69)	Positive 64 (65.31)	
Age (Years)	Mean±SD	48.36±11.28	-	-	-
	Median (Range)	48 (28–75)	-	-	
	≤40	27 (27.55)	7 (25.93)	20 (74.07)	0.2608
	>40	71 (72.45)	27 (38.03)	44 (61.97)	
Tumor size	>2–≤5 cm	67 (68.37)	23 (34.33)	44 (65.67)	0.8904
	>5 cm	18 (18.37)	7 (38.89)	11 (61.11)	
	≤2	13 (13.27)	4 (30.77)	9 (69.23)	
Lymph node metastasis	No	34 (34.69)	9 (26.47)	25 (73.53)	0.2126
	Yes	64 (65.31)	25 (39.06)	39 (60.94)	
Histological grading	Grade I	4 (4.08)	2 (50.00)	2 (50.00)	0.7385
	Grade II	41 (41.84)	13 (31.71)	28 (68.29)	
	Grade III	53 (54.08)	19 (35.85)	34 (64.15)	
Lymphovascular invasion	Negative	25 (25.77)	6 (24.00)	19 (76.00)	0.1789
	Positive	72 (74.23)	28 (38.89)	44 (61.11)	
Staging	Stage I	10 (10.20)	4 (40.00)	6 (60.00)	0.6946
	Stage II	49 (50.00)	15 (30.61)	34 (69.39)	
	Stage III	39 (39.80)	15 (38.46)	24 (61.54)	
ER	Negative	29 (29.59)	7 (24.14)	22 (75.86)	0.1547
	Positive	69 (70.41)	27 (39.13)	42 (60.87)	
PR	Negative	29 (29.59)	7 (24.14)	22 (75.86)	0.1547
	Positive	69 (70.41)	27 (39.13)	42 (60.87)	
HER2	Negative	68 (69.39)	26 (38.24)	42 (61.76)	0.2675
	Positive	30 (30.61)	8 (26.67)	22 (73.33)	
Ki-67 index (Cutoff 20%)	<20	45 (45.92)	20 (44.44)	25 (55.56)	0.0617
	≥20	53 (54.08)	14 (26.42)	39 (73.58)	
BC molecular subtypes	Luminal-A	38 (39.18)	18 (47.37)	20 (52.63)	0.2511
	Luminal-B Her2-ve	21 (21.65)	5 (23.81)	16 (76.19)	
	HER2-Enriched	19 (18.56)	4 (21.05)	15 (78.95)	
	Luminal-B Her2+ve	11 (11.34)	4 (36.36)	7 (63.64)	
	TNBC	9 (9.28)	3 (33.33)	6 (66.67)	
Progression event	No	59 (60.20)	24 (40.68)	35 (59.32)	0.1258
	Yes	39 (39.80)	10 (25.64)	29 (74.36)	
Local recurrence	No	87 (88.78)	33 (37.93)	54 (62.07)	0.0583
	Yes	11 (11.22)	1 (9.09)	10 (90.91)	
Distance metastasis	No	85 (86.73)	29 (34.12)	56 (65.88)	0.7593
	Yes	13 (13.27)	5 (38.46)	8 (61.54)	
Survival	Alive	70 (71.43)	27 (38.57)	43 (61.43)	0.2023
	Died	28 (28.57)	7 (25.00)	21 (75.00)	
OS in months	Mean±SD	78.26±30.03	-	-	-
	Median (Range)	53.3 (2.8–141.8)	-	-	-

ER: Estrogen receptor, PR: Progesterone receptor, HER2: Human epidermal growth factor receptor 2, OS: Overall survival

median of 82.03 months (MAD = 22.03), compared to HER2-Enriched subtypes, which had a median of 48.13 months (MAD = 21.07). Nonetheless, no statistically significant differences in time to progression were observed between the groups (p = 0.1616).

Local recurrence did not have a statistically significant impact on OS (p = 0.2418). However, patients without distant metastasis had a significantly longer median OS of 86.47 months (MAD = 16.87) compared to those with distant metastasis, whose median OS was 59.43 months (MAD = 25.66, p = 0.0009). In addition, patients with negative CD44s protein expression exhibited longer median OS (87.64 months, MAD = 13.7) and PFS (86.64 months, MAD = 18.14) compared to those with positive CD44s protein expression; nevertheless, the differences were not statistically significant (p = 0.1345 for OS, p = 0.0669 for PFS). Furthermore, no other clinicopathological prognostic factors were found to be significantly associated with OS or PFS in BC patients.

Fig. 2 shows Kaplan-Meier survival curves for OS and PFS of BC patients with respect to CD44s protein expression. Although patients with CD44-negative tumors demonstrated better prognosis and improved OS and PFS compared to those with CD44-positive tumors, the differences were not statistically significant. The median survival times were longer in the CD44-negative group, but the log-rank test yielded p-values of 0.1776 for OS and 0.2274 for PFS, respectively.

TABLE II
KAPLAN-MEIER (LOG-RANK TEST) ANALYSIS FOR OS AND PFS

Characteristics	Categories	OS in Months	p-value	PFS in Months	p-value
		Med (MAD)		Med (MAD)	
Age category	≤40	75.6 (16.23)	0.2104	72.33 (24.2)	0.4105
	>40	86.47 (17.5)		72.57 (25.9)	
Tumor size	>2–≤5 cm	86.47 (15.86)	**0.0229**	75.27 (20.5)	**0.0023**
	>5 cm	53.42 (25.39)		17.85	
	≤2 cm	86.7 (18.53)		86.7 (18.53)	
Lymph node metastasis	No	85.52 (15.42)	0.2224	74.84 (18.52)	0.2085
	Yes	81.53 (20.22)		70.12 (27.15)	
Histological grading	I	80.85 (9.83)	0.8578	80.85 (9.83)	0.4466
	II	81.03 (16.56)		75.3 (20.83)	
	III	86.33 (19.14)		69.4 (29.07)	
Lymphovascular invasion	Negative	72.57 (12.7)	0.4529	72.57 (13.9)	0.3664
	Positive	86.4 (19.27)		72.44 (29.09)	
Staging	I	87.05 (20.44)	0.1017	87.05 (20.44)	**0.0199**
	II	86.47 (15.07)		75.3 (20.47)	
	III	75.27 (30.6)		59.63 (26.7)	
ER	Negative	69.4 (26.37)	**0.0198**	61.23 (26.2)	**0.0392**
	Positive	86.33 (15.7)		75.9 (22.37)	
PR	Negative	69.4 (26.37)	**0.0198**	61.23 (26.2)	**0.0392**
	Positive	86.33 (15.7)		75.9 (22.37)	
HER2	Negative	86.215 (14.89)	0.1269	78.47 (19.79)	0.1030
	Positive	70.04 (28.01)		59.67 (26.3)	
Ki-67 index (Cutoff 20%)	<20%	85.33 (19.57)	0.5493	75.9 (23.23)	0.1802
	≥20%	82.03 (15.87)		69.4 (26.37)	
BC molecular subtypes	Luminal-B Her2-ve	87.4 (11.4)	0.0982	82.03 (22.03)	0.1616
	Luminal-B Her2+ve	86.47 (27.56)		75.3 (38.73)	
	Luminal-A	85.83 (16.37)		78.47 (20.52)	
	TNBC	73.77 (18.06)		73.77 (18.06)	
	HER2-Enriched	68.5 (27.27)		48.13 (21.07)	
Local recurrence	No	82.03 (16.83)	0.2418	-	-
	Yes	86.47 (19.4)		-	
Distance metastasis	No	86.47 (16.87)	**0.0009**	-	-
	Yes	59.43 (25.66)		-	
CD44s protein expression	Negative	87.64 (13.7)	0.1345	86.64 (18.14)	0.0669
	Positive	75.75 (21.09)		69.54 (26)	

MAD: Median absolute deviation, ER: Estrogen receptor, PR: Progesterone receptor, HER2: Human epidermal growth factor receptor 2, OS: Overall survival, PFS: Progression-free survival. The bold values indicate p-values < 0.05.

E. Cox Regression Analysis of Survival in BC Patients

In the present study, patients with LVI had a 2.37-fold higher risk of death compared to those without LVI, making it the only significant predictor of poor OS (HR = 2.37, 95% CI = 1.06–5.29; p = 0.036). LVI-positive tumors also showed a higher risk of progression (HR = 2.19, 95% CI = 0.95–5.03), though this did not reach statistical significance (p = 0.064) (Table III).

Although patients with Stage II disease exhibited a higher risk of progression (HR = 3.28, 95% CI = 0.75–14.28), the association was not statistically significant (p = 0.122). A tumor size greater than 5 cm also showed worse survival outcomes for both OS (HR = 1.74, 95% CI = 0.37–8.21) and PFS (HR = 1.97, 95% CI = 0.37–10.47), yet the associations were not statistically significant (OS: p = 0.701; PFS: p = 0.709). Finally, other variables (e.g., ER status, lymph node metastasis, age, HER2, Ki-67, CD44s protein expression) did not show significant correlations with survival (all p > 0.05).

IV. DISCUSSION

In this study, IHC analysis using AI-based scoring methods was employed to investigate the expression of CD44s cell membrane protein in BC patients and its potential prognostic value. Our analysis revealed that 65.31% of patients exhibited positive CD44s protein expression, while 34.69% were negative, consistent with previous studies on CSC markers in BC tissues (Mohamed, et al., 2019; Wu, et al., 2015). However, despite the high rate of CD44s protein expression, we found no significant correlation between CD44s protein expression and key clinicopathological factors such as age, tumor size, lymph node metastasis, or hormone receptor status. The lack of association with clinicopathological factors aligns with studies reporting no significant correlation between CD44s protein expression and clinical outcomes (Abraham, et al., 2005). This may suggest that the standard isoform of CD44 cell membrane protein contributes to tumor initiation, warranting further

http://dx.doi.org/10.14500/aro.12248

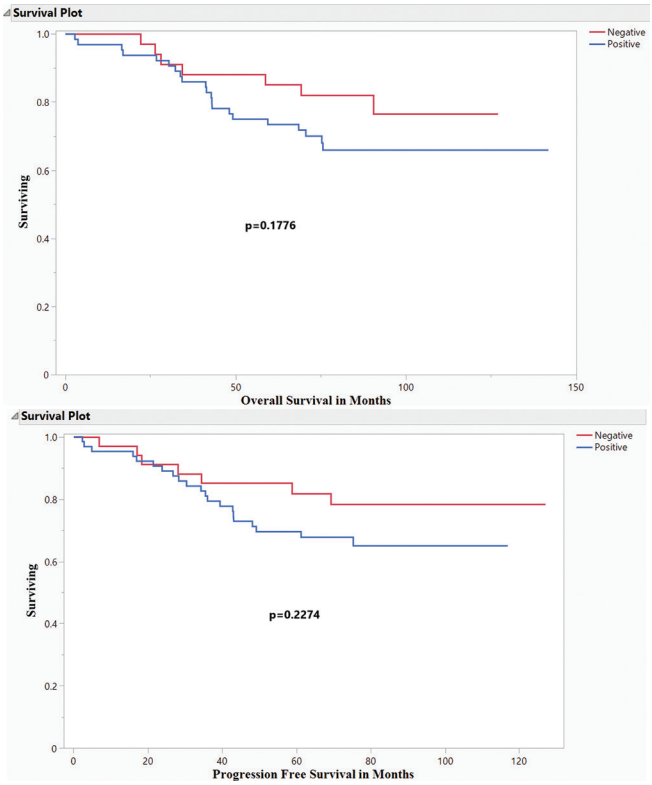

Fig. 2. Kaplan-Meier survival curves with log-rank test results. Comparison of overall survival between patients with positive and negative CD44s protein expression (top); comparison of progression-free survival between patients with positive and negative CD44s protein expression (bottom).

investigation into its role in both primary and metastatic tissues in BC patients.

Nevertheless, conflicting results from other studies regarding the association of CD44s with clinicopathological characteristics highlight the complexity of CD44s as a prognostic and predictive biomarker (Wu, et al., 2015). These discrepancies may be due to differences in study populations, methodologies, or the biological heterogeneity of BC subtypes. Furthermore, the specific CD44 isoform selected in various studies may demonstrate distinct roles in BC initiation and progression (Yang, et al., 2019; Brown, et al., 2011; Guo, et al., 2021).

Kaplan-Meier survival analysis showed that CD44s protein expression did not significantly affect OS or DFS, which may be due to the short follow-up period of the cohort. Notably, similar clinical outcomes were reported in a study by Abraham, et al. (Abraham, et al., 2005). However, a meta-analysis suggested that CD44 serves as a negative prognostic marker for OS and PFS (Gu, et al., 2022). It is possible that CD44v isoforms play a more prominent role in BC progression (Hu, et al., 2017). Since our study focused on CD44s, future research should include CD44v isoforms and a larger cohort to better clarify the prognostic significance of CD44.

Interestingly, our analysis identified LVI as the only independent predictor of both OS and PFS, underscoring its importance as a key prognostic factor in BC. This finding aligns with other studies that have associated LVI with more aggressive BC subtypes, higher recurrence rates, and lower survival outcomes (Lee, et al., 2023; Nishimura, et al., 2022; Song, et al., 2011).

TABLE III
Cox regression Analysis for OS and PFS in BC Patients

Predictors (n=98)	OS in months		PFS in Months	
	HR (95% CI)	p-value	HR (95% CI)	p-value
Age category		0.37404		0.78630
>40 versus ≤40	0.74 (0.38–1.43)		1.10 (0.56–2.16)	
Tumor size		0.70059		0.70915
>2–≤5 cm versus ≤2	1.64 (0.50–5.33)		1.36 (0.40–4.61)	
>5 cm versus ≤2	1.74 (0.37–8.21)		1.97 (0.37–10.47)	
Lymph node metastasis		0.34261		0.55337
Yes versus No	1.50 (0.65–3.47)		1.31 (0.54–3.18)	
Histological grading		0.60362		0.77761
II versus I	0.82 (0.25–2.65)		0.79 (0.24–2.56)	
III versus I	0.59 (0.16–2.19)		0.64 (0.17–2.41)	
Lymphovascular invasion		**0.03565**		0.06433
Positive versus Negative	2.37 (1.06–5.29)		2.19 (0.95–5.03	
Staging		0.50417		0.12226
II versus I	1.92 (0.50–7.31)		3.28 (0.75–14.28)	
III versus I	1.51 (0.28–8.28)		2.19 (0.36–13.39)	
ER		0.31812		0.81644
Positive versus Negative	0.66 (0.29–1.49)		0.91 (0.41–2.03)	
PR		0.31812		0.81644
Positive versus Negative	0.66 (0.29–1.49)		0.91 (0.41–2.03)	
HER2		0.80453		0.90197
Positive versus Negative	1.15 (0.39–3.36)		0.93 (0.31–2.84)	
Ki-67 (20%)		0.95403		0.73258
≥20% versus <20%	1.02 (0.50–2.10)		1.13 (0.56–2.30)	
CD44s protein expression		0.99849		0.95663
Positive versus Negative	1.00 (0.54–1.86)		0.98 (0.51–1.90)	

ER: Estrogen receptor, PR: Progesterone receptor, HER2: Human epidermal growth factor receptor 2, OS: Overall survival, PFS: Progression-free survival

The integration of an AI-based scoring method for IHC slide quantification represents a significant advancement in BC diagnostics. In this study, we observed moderate agreement between the AI-based scoring method and manual scoring of CD44s cell membrane protein expression, highlighting the potential of AI to complement traditional approaches, particularly in reducing interobserver variability.

Despite its strengths, this study has several limitations. These include its retrospective design, relatively short follow-up period, and relatively small sample size, particularly within stratified subgroups, which may limit the statistical power to detect subtle associations. Another potential limitation is recall bias, especially for data obtained directly from patients. However, most clinical and follow-up information was sourced from hospital records, including patient registries, the oncology clinic, and the cancer center database at Azadi Teaching Hospital, helping to reduce this risk. For the small portion of data collected through patient phone calls, no more practical or reliable method was available. Future studies should aim to validate these findings in larger, prospective cohorts and explore the distinct roles of CD44s and CD44v isoforms in BC progression and survival outcomes. Moreover, the development and refinement of AI-based scoring systems warrant further exploration to establish standardized protocols for clinical application.

V. Conclusion

This study contributes to the growing body of literature on CD44s cell membrane protein expression in BC, providing insights into its role in disease characterization. While some results align with prior studies, others contradict established findings, underscoring the complexity of CD44s cell membrane protein expression as a biomarker. Future research with larger cohorts and integrated molecular profiling is needed to clarify the prognostic and therapeutic relevance of CD44s cell membrane protein expression in BC. The moderate concordance between AI-based and manual scoring methods highlights the promise of AI in enhancing pathological assessments. Further research is essential to elucidate the prognostic value of CD44s cell membrane protein expression and to optimize AI tools alongside manual pathology, ensuring robustness and accuracy for routine clinical use.

REFERENCES

Abraham, B.K., Fritz, P., McClellan, M., Hauptvogel, P., Athelogou, M., and Brauch, H., 2005. Prevalence of CD44+/CD24−/low cells in breast cancer may not be associated with clinical outcome but may favour distant metastasis. *Clinical Cancer Research*, 11(3), pp.1154-1159.

Acs, B., Pelekanou, V., Bai, Y., Martinez-Morilla, S., Toki, M., Leung, S.C., Nielsen, T.O., and Rimm, D.L., 2019. Ki-67 reproducibility using digital image analysis: An inter-platform and inter-operator study. *Laboratory Investigation*, 99(1), pp.107-117.

Aeffner, F., Adissu, H.A., Boyle, M.C., Cardiff, R.D., Hagendorn, E., Hoenerhoff, M.J., Klopfleisch, R., Newbigging, S., Schaudien, D., Turner, O., and Wilson, K., 2018. Digital microscopy, image analysis, and virtual slide repository. *ILAR journal*, 59(1), pp.66-79.

Al-Hajj, M., Wicha, M.S., Benito-Hernandez, A., Morrison, S.J., and Clarke, M.F., 2003. Prospective identification of tumorigenic breast cancer cells. *Proceedings of the National Academy of Sciences*, 100(7), pp.3983-3988.

Barnard, M.E., Boeke, C.E., and Tamimi, R.M., 2015. Established breast cancer risk factors and risk of intrinsic tumour subtypes. *Biochimica Biophysica Acta (BBA)-Reviews on Cancer*, 1856(1), pp.73-85.

Bei, Y., Cheng, N., Chen, T., Shu, Y., Yang, Y., Yang, N., Zhou, X., Liu, B., Wei, J., Liu, Q., Zheng, W., Zhang, W., Su, H., Zhu, W., Ji, J., and Shen, P., 2020. CDK5 inhibition abrogates TNBC stem□cell property and enhances anti□PD□1 therapy. *Advanced Science*, 7(22), p.2001417.

Braun, M., Piasecka, D., Bobrowski, M., Kordek, R., Sadej, R., and Romanska, H.M., 2020. A 'Real-Life'experience on automated digital image analysis of FGFR2 immunohistochemistry in breast cancer. *Diagnostics(Basel)*, 10(12), p.1060.

Bray, F., Laversanne, M., Sung, H., Ferlay, J., Siegel, R.L., Soerjomataram, I., and Jemal, A., 2024. Global cancer statistics 2022: GLOBOCAN estimates of incidence and mortality worldwide for 36 cancers in 185 countries. *CA: A Cancer Journal for Clinicians*, 74(3), pp.229-263.

Brown, R.L., Reinke, L.M., Damerow, M.S., Perez, D., Chodosh, L.A., Yang, J., and Cheng, C., 2011. CD44 splice isoform switching in human and mouse epithelium is essential for epithelial-mesenchymal transition and breast cancer progression. *The Journal of Clinical Investigation*, 121(3), pp.1064-1074.

Bustreo, S., Osella-Abate, S., Cassoni, P., Donadio, M., Airoldi, M., Pedani, F., Papotti, M., Sapino, A., and Castellano, I., 2016. Optimal Ki-67 cut-off for luminal breast cancer prognostic evaluation: A large case series study with a long-term follow-up. *Breast Cancer Research and Treatment*, 157, pp.363-371.

Cho, Y., Lee, H.W., Kang, H.G., Kim, H.Y., Kim, S.J., and Chun, K.H., 2015. Cleaved CD44 intracellular domain supports activation of stemness factors and promotes tumorigenesis of breast cancer. *Oncotarget*, 6(11), pp.8709-8721.

Clark, G.C., Hampton, J.D., Koblinski, J.E., Quinn, B., Mahmoodi, S., Metcalf, O., Guo, C., Peterson, E., Fisher, P.B., Farrell, N.P., Wang, X.Y., and Mikkelsen, R.B., 2022. Radiation induces ESCRT pathway dependent CD44v3+ extracellular vesicle production stimulating pro-tumor fibroblast activity in breast cancer. *Frontiers in Oncology*, 12, p.913656.

Dai, X., Li, T., Bai, Z., Yang, Y., Liu, X., Zhan, J., and Shi, B., 2015. Breast cancer intrinsic subtype classification, clinical use and future trends. *American Journal of Cancer Research*, 5(10), pp.2929-2943.

Elston, C.W., and Ellis, I.O., 1991. Pathological prognostic factors in breast cancer. I. The value of histological grade in breast cancer: Experience from a large study with long□term follow□up. *Histopathology*, 19(5), pp.403-410.

Giuliano, A.E., Edge, S.B., and Hortobagyi, G.N., 2018. Eighth edition of the AJCC cancer staging manual: Breast cancer. *Annals of Surgical Oncology*, 25, pp.1783-1785.

Gong, Y., Sun, X., Huo, L., Wiley, E.L., and Rao, M.S., 2005. Expression of cell adhesion molecules, CD44s and E□cadherin, and microvessel density in invasive micropapillary carcinoma of the breast. *Histopathology*, 46(1), pp.24-30.

Goodison, S., Urquidi, V., and Tarin, D., 1999. CD44 cell adhesion molecules. *Molecular Pathology*, 52(4), pp.189-196.

Gu, J., Chen, D., Li, Z., Yang, Y., Ma, Z., and Huang, G., 2022. Prognosis assessment of $CD44^{+}/CD24^{-}$ in breast cancer patients: A systematic review and meta-analysis. *Archives of Gynecology and Obstetrics*, 306(4), pp.1147-1160.

Guo, Q., Liu, Y., He, Y., Du, Y., Zhang, G., Yang, C., and Gao, F., 2021. CD44 activation state regulated by the CD44v10 isoform determines breast cancer proliferation. *Oncology Reports*, 45(4), p.7.

Herrera-Gayol, A., and Jothy, S., 1999. Adhesion proteins in the biology of breast cancer: Contribution of CD44. *Experimental and Molecular Pathology*, 66(2), pp.149-156.

Hu, J., Li, G., Zhang, P., Zhuang, X., and Hu, G., 2017. A CD44v+ subpopulation of breast cancer stem-like cells with enhanced lung metastasis capacity. *Cell Death Disease*, 8(3), p.e2679.

Lee, K., Kruper, L., Dieli-Conwright, C.M., and Mortimer, J.E., 2019. The impact of obesity on breast cancer diagnosis and treatment. *Current Oncology Reports*, 21, p.41.

Lee, S.J., Go, J., Ahn, B.S., Ahn, J.H., Kim, J.Y., Park, H.S., Kim, S.I., Park, B.W., and Park, S., 2023. Lymphovascular invasion is an independent prognostic factor in breast cancer irrespective of axillary node metastasis and molecular subtypes. *Frontiers in Oncology*, 13, p.1269971.

Liu, Y., Han, D., Parwani, A.V., and Li, Z., 2023. Applications of artificial intelligence in breast pathology. *Archives of Pathology and Laboratory Medicine*, 147(9), pp.1003-1013.

Lopez, J.I., Camenisch, T.D., Stevens, M.V., Sands, B.J., McDonald, J., and Schroeder, J.A., 2005. CD44 attenuates metastatic invasion during breast cancer progression. *Cancer Research*, 65(15), pp.6755-6763.

McCaffrey, C., Jahangir, C., Murphy, C., Burke, C., Gallagher, W.M., and Rahman, A., 2024. Artificial intelligence in digital histopathology for predicting patient prognosis and treatment efficacy in breast cancer. *Expert Review of Molecular Diagnostics*, 24(5), pp.363-377.

Mohamed, S.Y., Kaf, R.M., Ahmed, M.M., Elwan, A., Ashour, H.R., and Ibrahim, A., 2019. The prognostic value of cancer stem cell markers (Notch1, ALDH1, and CD44) in primary colorectal carcinoma. *Journal of Gastrointestinal Cancer*, 50, pp.824-837.

Nishimura, R., Osako, T., Okumura, Y., Nakano, M., Ohtsuka, H., Fujisue, M., and Arima, N., 2022. An evaluation of lymphovascular invasion in relation to biology and prognosis according to subtypes in invasive breast cancer. *Oncology Letters*, 24(2), p.245.

Pati, P., Karkampouna, S., Bonollo, F., Compérat, E., Radić, M., Spahn, M., Martinelli, A., Wartenberg, M., Kruithof-de Julio, M., and Rapsomaniki, M., 2024. Accelerating histopathology workflows with generative AI-based virtually multiplexed tumor profiling. *Nature Machine Intelligence*, 6(9), pp.1077-1093.

Paulsen, I.M.S., Dimke, H., and Frische, S., 2015. A single simple procedure for dewaxing, hydration and heat-induced epitope retrieval (HIER) for immunohistochemistry in formalin fixed paraffin-embedded tissue. *European Journal of Histochemistry EJH*, 59(4), p.2532.

Rakha, E.A., Vougas, K., and Tan, P.H., 2022. Digital technology in diagnostic breast pathology and immunohistochemistry. *Pathobiology*, 89(5), pp.334-342.

Schmitt, F., Ricardo, S., Vieira, A.F., Dionísio, M.R., and Paredes, J., 2012. Cancer stem cell markers in breast neoplasias: Their relevance and distribution in distinct molecular subtypes. *Virchows Archiv*, 460, pp.545-553.

Senbanjo, L.T., and Chellaiah, M.A., 2017. CD44: A multifunctional cell surface adhesion receptor is a regulator of progression and metastasis of cancer cells. *Frontiers in Cell and Developmental Biology*, 5, p.18.

Somal, P.K., Sancheti, S., Sharma, A., Sali, A.P., Chaudhary, D., Goel, A., Dora, T.K., Brar, R., Gulia, A., and Divatia, J., 2023. A clinicopathological analysis of molecular subtypes of breast cancer using immunohistochemical surrogates: A 6-year institutional experience from a tertiary cancer center in north India. *South Asian Journal of Cancer*, 12(02), pp.104-111.

Song, Y.J., Shin, S.H., Cho, J.S., Park, M.H., Yoon, J.H., and Jegal, Y.J., 2011. The role of lymphovascular invasion as a prognostic factor in patients with lymph node-positive operable invasive breast cancer. *Journal of Breast Cancer*, 14(3), pp.198-203.

Steinbichler, T.B., Dudás, J., Skvortsov, S., Ganswindt, U., Riechelmann, H., and Skvortsova, I.I., 2018. December. Therapy resistance mediated by cancer stem cells. In: *Seminars in Cancer Biology.* Vol. 53. Academic Press, United States, pp.156-167.

Turner, K.M., Yeo, S.K., Holm, T.M., Shaughnessy, E., and Guan, J.L., 2021. Heterogeneity within molecular subtypes of breast cancer. *American Journal of Physiology Cell Physiology*, 321(2), pp.C343-C354.

Vadhan, A., Hou, M.F., Vijayaraghavan, P., Wu, Y.C., Hu, S.C.S., Wang, Y.M., Cheng, T.L., Wang, Y.Y., and Yuan, S.S.F., 2022. CD44 promotes breast cancer metastasis through AKT-mediated downregulation of nuclear FOXA2. *Biomedicines*, 10(10), p.2488.

Vallejos, C.S., Gómez, H.L., Cruz, W.R., Pinto, J.A., Dyer, R.R., Velarde, R., Suazo, J.F., Neciosup, S.P., León, M., De La Cruz, M.A., and Vigil, C.E., 2010. Breast cancer classification according to immunohistochemistry markers: Subtypes and association with clinicopathologic variables in a peruvian hospital database. *Clinical Breast Cancer*, 10(4), pp.294-300.

Walcher, L., Kistenmacher, A.K., Suo, H., Kitte, R., Dluczek, S., Strauß, A., Blaudszun, A.R., Yevsa, T., Fricke, S., and Kossatz-Boehlert, U., 2020. Cancer stem cells-origins and biomarkers: Perspectives for targeted personalized therapies. *Frontiers in Immunology*, 11, p.1280.

Wilson, M.M., Weinberg, R.A., Lees, J.A., and Guen, V.J., 2020. Emerging mechanisms by which EMT programs control stemness. *Trends in Cancer*, 6(9), pp.775-780.

Winters, S., Martin, C., Murphy, D., and Shokar, N.K., 2017. Breast cancer epidemiology, prevention, and screening. *Progress in Molecular Biology and Translational Science*, 151, pp.1-32.

Wu, Q., Yang, Y., Wu, S., Li, W., Zhang, N., Dong, X., and Ou, Y., 2015. Evaluation of the correlation of KAI1/CD82, CD44, MMP7 and β-catenin in the prediction of prognosis and metastasis in colorectal carcinoma. *Diagnostic Pathology*, 10, p.176.

Wu, S., Yue, M., Zhang, J., Li, X., Li, Z., Zhang, H., Wang, X., Han, X., Cai, L., Shang, J., Jia, Z., Wang, X., Li, J., and Liu, Y., 2023. The role of artificial intelligence in accurate interpretation of HER2 immunohistochemical scores 0 and 1+ in breast cancer. *Modern Pathology*, 36(3), p.100054.

Wu, X.J., Li, X.D., Zhang, H., Zhang, X., Ning, Z.H., Yin, Y.M., and Tian, Y., 2015. Clinical significance of CD44s, CD44v3 and CD44v6 in breast cancer. *Journal of International Medical Research*, 43(2), pp.173-179.

Xiong, X., Zheng, L.W., Ding, Y., Chen, Y.F., Cai, Y.W., Wang, L.P., Huang, L., Liu, C.C., Shao, Z.M., and Yu, K.D., 2025. Breast cancer: Pathogenesis and treatments. *Signal Transduction and Targeted Therapy*, 10(1), p.49.

Yang, C., Cao, M., Liu, Y., He, Y., Du, Y., Zhang, G., and Gao, F., 2019. Inducible formation of leader cells driven by CD44 switching gives rise to collective invasion and metastases in luminal breast carcinomas. *Oncogene*, 38(46), pp.7113-7132.

Zahwe, M., Bendahhou, K., Eser, S., Mukherji, D., Fouad, H., Fadhil, I., Soerjomataram, I., and Znaor, A., 2025. Current and future burden of female breast cancer in the Middle East and North Africa region using estimates from GLOBOCAN 2022. *International Journal of Cancer*, 156, pp.2320-2329.

Zhang, H., Brown, R.L., Wei, Y., Zhao, P., Liu, S., Liu, X., Deng, Y., Hu, X., Zhang, J., Gao, X.D., Kang, Y., Mercurio, A.M., Goel, H.L., and Cheng, C., 2019. CD44 splice isoform switching determines breast cancer stem cell state. *Genes and Development*, 33(3-4), pp.166-179.